

# Structural Basis for the Guanosine Requirement of the Hairpin Ribozyme<sup>†</sup>

Robert Pinard,<sup>‡</sup> Dominic Lambert,<sup>§</sup> Nils G. Walter,<sup>‡</sup> Joyce E. Heckman,<sup>‡</sup> François Major,<sup>§</sup> and John M. Burke<sup>\*,‡</sup>

*Department of Microbiology and Molecular Genetics, University of Vermont, 306 Stafford Hall, Burlington, Vermont 05405, and Département d'informatique et Recherche Opérationnelle, Université de Montréal, 2920 chemin de la tour, C.P.6128, Succ. centre-ville, Montréal, Québec H3C 3J7, Canada*

*Received August 30, 1999; Revised Manuscript Received September 29, 1999*

**ABSTRACT:** To form a catalytically active complex, the essential nucleotides of the hairpin ribozyme, embedded within the internal loops of the two domains, must interact with one another. Little is known about the nature of these essential interdomain interactions. In the work presented here, we have used recent topographical constraints and other biochemical data in conjunction with molecular modeling (constraint-satisfaction program MC-SYM) to generate testable models of interdomain interactions. Visual analysis of the generated models has revealed a potential interdomain base pair between the conserved guanosine immediately downstream of the reactive phosphodiester ( $G_{+1}$ ) and  $C_{25}$  within the large domain. We have tested this former model through activity assays, using all 16 combinations of bases at positions +1 and 25. When the standard ribozyme was used, catalytic activity was severely suppressed with substrates containing  $U_{+1}$ ,  $C_{+1}$ , or  $A_{+1}$ . Similarly, mutations of the putative pairing partner ( $C_{25}$  to  $A_{25}$  or  $G_{25}$ ) reduce activity by several orders of magnitude. The  $U_{25}$  substitution retains a significant level of activity, consistent with the possible formation of a G·U wobble pair. Strikingly, when combinations of Watson–Crick (or wobble) base pairs were introduced in these positions, catalytic activity was restored, strongly suggesting the existence of the proposed interaction. These results provide a structural basis for the guanosine requirement of this ribozyme and indicate that the hairpin ribozyme can now be engineered to cleave a wider range of RNA sequences.

The hairpin ribozyme is a small catalytic RNA motif isolated from the minus strand of the tobacco ringspot virus satellite RNA. It acts as an endonuclease that catalyzes a reversible sequence-specific cleavage reaction within a substrate RNA (1). The hairpin ribozyme–substrate complex contains two independently folding domains (2). Several studies indicate that tertiary interactions between conserved segments of the two domains are required to form a catalytically active complex (2–6).

There is no X-ray crystal or complete NMR structure for the hairpin ribozyme (7, 8), and until recently, very few interdomain constraints have been available to guide modeling efforts. Recent cross-links obtained by disulfide linkages (9) and topographical constraints obtained in our laboratory using hydroxyl radical footprinting and photoaffinity cross-linking (10, 11) have provided important information concerning the alignment of the two domains in the docked state. However, little is known about the key structural elements involved in the tertiary interactions between the two domains. The guanosine ( $G_{+1}$ ) immediately downstream of the cleavage/ligation site represents a potential candidate for an interdomain contact, since the RNA cleavage and ligation

reactions catalyzed by the hairpin ribozyme exhibit a strong requirement for this nucleotide (12). Base substitutions at this site reduce catalytic activity by several orders of magnitude, and inhibit the formation of a stable tertiary complex between the two domains of the ribozyme–substrate complex (12, 13). NMR analysis of the isolated substrate-binding domain shows a sheared  $G_{+1}\cdot A_9$  base pair, while the Watson–Crick face of  $G_{+1}$  is unoccupied (7). Finally,  $G_{+1}$  and surrounding nucleotides at the cleavage/ligation site are protected from hydroxyl radical cleavage upon docking of the two domains, with concomitant protection of nucleotides 25–27 within the large domain, and the same regions of the complex have been photochemically cross-linked (10, 11).

In the work presented here, we have used three-dimensional computer modeling using MC-SYM, compensatory base substitutions, and FRET<sup>1</sup> to identify and investigate a potential Watson–Crick base pair between  $G_{+1}$  and the cytosine at position 25. This methodology is one of the few examples of the application of RNA modeling methods based on constraints derived from biochemical data in correctly modeling and then experimentally demonstrating a specific RNA tertiary interaction.

## EXPERIMENTAL PROCEDURES

*Preparation of RNA Oligonucleotides.* RNA was synthesized using solid-phase phosphoramidite chemistry and

<sup>†</sup> This work was supported by grants from the National Institutes of Health (AI 44186) to J.M.B. and from the Medical Research Council of Canada (MT 14504) to F.M. R.P. was supported by a postdoctoral fellowship from the Medical Research Council of Canada.

\* To whom correspondence should be addressed. Telephone: (802) 656-8503. Fax: (802) 656-8749. E-mail: John.Burke@uvm.edu.

<sup>‡</sup> University of Vermont.

<sup>§</sup> Université de Montréal.

<sup>1</sup> Abbreviation: FRET, fluorescence resonance energy transfer.

purified as described previously (14). RNA phosphoramidites were purchased from Glen Research, Inc. (Sterling, VA).

**Cleavage Assays.** The ribozyme–substrate complexes were reconstituted by incubating the ribozyme segments (100 nM) in standard reaction buffer [50 mM Tris-HCl (pH 7.5) and 12 mM MgCl<sub>2</sub> or 50 mM Tris-HCl (pH 7.5) and 1 mM Co(NH<sub>3</sub>)<sub>6</sub><sup>3+</sup>] for 20 min at 37 °C. Cleavage reactions were initiated by addition of 1 nM 5′-<sup>32</sup>P-end-labeled substrate RNA and performed at 25 °C. Measurements were taken by quenching aliquots of the reaction with 10 volumes of 90% formamide and 15 mM EDTA during a 60 min period for qualitative assays and over time courses extending to 120–300 min for determination of cleavage rates.

**Docking Assays.** Docking of the substrate-binding and large domains of the hairpin ribozyme–substrate complex was detected by following fluorescence resonance energy transfer between a domain-terminal donor–acceptor fluorophore pair as described previously (13). Doubly labeled ribozyme (50 nM) was preincubated in 50 mM Tris-HCl (pH 7.5), 12 mM MgCl<sub>2</sub>, and 25 mM DTT at 25 °C for 15 min before a 10-fold excess of substrate was manually added for rapid binding and initiation of domain docking. Fluorescein was excited at 485 nm; fluorescence emission was monitored at both 515 nm (for the fluorescein donor) and 560 nm (for the hexachlorofluorescein acceptor), and a normalized  $F_{560}/F_{515}$  ratio was calculated as a function of time.

**Modeling of the Catalytic Core Using MC-SYM.** The structural constraints for defining an MC-SYM script for the hairpin ribozyme catalytic core were derived from the secondary structure, cross-linking, and biochemical data shown in Figure 1 and other unpublished photochemical constraints (J. E. Heckman and J. M. Burke, unpublished observations). An A-RNA structure was assumed for all helices. The C2′-endo conformation was assigned to the G<sub>+1</sub> residue, and all possible conformations were tested, including pucker modes and glycosyl angles for the nucleotides of the loop regions. To reduce the number of generated models, conformational assignments in the loops were limited and similar generated solutions (2 Å difference) were combined by MC-SYM. The MC-SYM script is available on request or at [www-lbit.iro.umontreal.ca/McSym\\_Repository/HairpinRibozyme\\_lambert\\_14-04-99.mcc](http://www-lbit.iro.umontreal.ca/McSym_Repository/HairpinRibozyme_lambert_14-04-99.mcc).

## RESULTS AND DISCUSSION

Models of the catalytic core of the ribozyme–substrate complex were generated using the constraint-satisfaction program MC-SYM (15, 16). Loose application of five azidophenacyl cross-links (11) (distance spanned by each cross-link being  $\geq 15$  Å) and two stacking constraints from photochemical cross-linking (unpublished data) resulted in  $>10^5$  structures, while fewer than  $10^2$  models were obtained when all the cross-linking constraints were provided simultaneously to MC-SYM and the average distance for the azidophenacyl cross-links was limited to 7.5–15 Å (the approximate length of the cross-linking agent used in our previous study). These topographical constraints introduced a sharp bend within the substrate, in agreement with the ability of the hairpin ribozyme to cleave short circular substrates (J. A. Esteban, Z. S. Taylor, and J. M. Burke, manuscript in preparation). Visual inspection revealed plau-

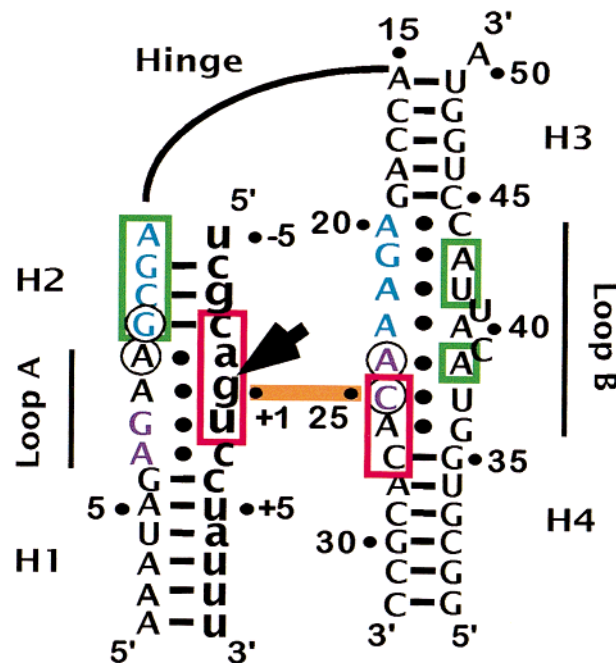


FIGURE 1: Secondary structure of the hairpin ribozyme–substrate complex. Interactions within internal loops A and B are as described previously (7, 8). Red and green rectangles indicate pairs of areas of the ribose–phosphate backbone protected upon domain docking and which are proposed to interact in the docked complex (10). Blue and lilac nucleotides indicate pairs of regions of the ribozyme that have been photochemically cross-linked (11). The circled nucleotides indicate the positions of the 2′-hydroxyl groups implicated in docking (22) and proposed to be involved in the formation of a ribose zipper between the two domains (9). The positions of nucleotides involved in the proposed Watson–Crick base pair (G<sub>+1</sub> and C<sub>25</sub>) are indicated by an orange line, and the cleavage/ligation site is indicated by a black arrow. The four helical segments are numbered H1–H4. Substrate is represented in lowercase letters.

sible interactions between C<sub>25</sub> and either G<sub>+1</sub> or U<sub>37</sub> in several models. Base and nucleotide residue substitutions fit the G<sub>+1</sub>·C<sub>25</sub> model but are inconsistent with C<sub>25</sub>·U<sub>37</sub> (17, 18); therefore, we used mutational analysis to test the former model.

The G<sub>+1</sub>·C<sub>25</sub> model was tested through activity assays employing all 16 combinations of natural bases at positions +1 and 25 (Figure 2). In agreement with previous results (12), using the standard ribozyme, the catalytic activity is severely suppressed with substrates containing U<sub>+1</sub>, C<sub>+1</sub>, or A<sub>+1</sub>, in the presence of either 12 mM MgCl<sub>2</sub> or 1 mM cobalt(III) hexammine ( $k_{\text{cleave}} < 10^{-5}$  min<sup>-1</sup>), and higher concentrations of ribozymes and metal ions did not restore activity. Similarly, mutations of the putative pairing partner (C<sub>25</sub> to A<sub>25</sub> or G<sub>25</sub>) reduce activity by at least 5 orders of magnitude. Notably, the G<sub>+1</sub>·U<sub>25</sub> combination retains significant activity, consistent with the possibility of a G·U wobble pair. Strikingly, the U<sub>25</sub> ribozyme has greater activity against the A<sub>+1</sub> substrate than against the G<sub>+1</sub> substrate. Using the two-way junction ribozyme construct of Figure 1 in Mg<sup>2+</sup>-containing buffers, the A<sub>+1</sub>·U<sub>25</sub> cleaves at a rate only 1 order of magnitude slower than that of G<sub>+1</sub>·C<sub>25</sub>. Moderate compensation is seen in the C<sub>+1</sub>·G<sub>25</sub> variant, while low but significant activity is observed for U<sub>+1</sub>·A<sub>25</sub>. Previous experiments in our laboratory using FRET have shown that a G to A mutation at the +1 position does not significantly

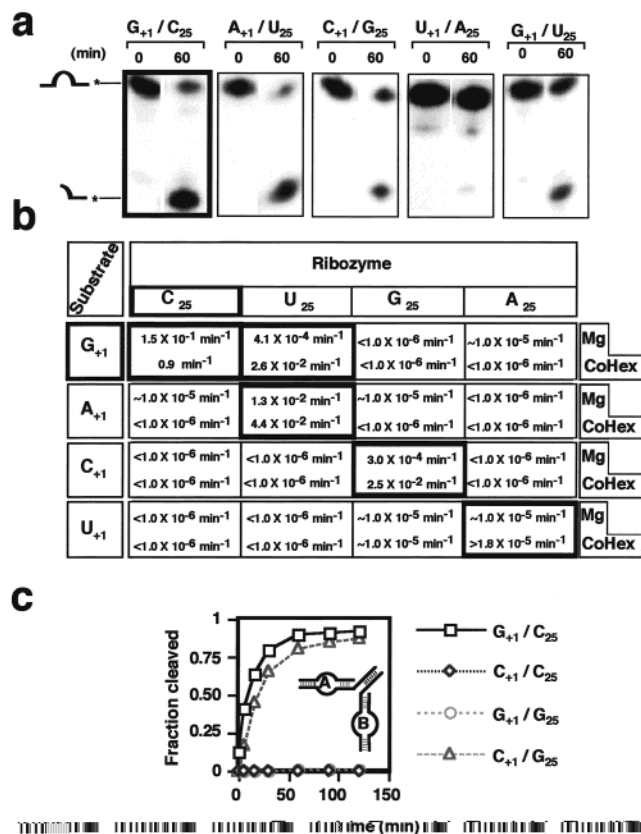


FIGURE 2: Cleavage activity of variant ribozymes representing single-base changes at positions 25. (a) Example of restoration of cleavage activity obtained in the presence of 1 mM Co(NH<sub>3</sub>)<sub>6</sub>Cl<sub>3</sub>. The assembled ribozymes were assayed for cleavage activity using 5'-labeled substrates with or without a substitution at the +1 position. Full-length and cleaved substrates are indicated on the right. The variant combinations and the time points are indicated on top of each autoradiograph. The bold rectangle indicates the wild-type combination. (b) Cleavage rates obtained for the 16 combinations of bases at positions +1 and 25. The first row of each combination indicates the first-order cleavage rate observed in the presence of 12 mM MgCl<sub>2</sub> and the second row in the presence of 1 mM Co(NH<sub>3</sub>)<sub>6</sub>Cl<sub>3</sub>. The combinations allowing significant cleavage activity are indicated by bold rectangles. (c) Example of the cleavage activity restoration that can be achieved when reaction conditions [1 mM Co(NH<sub>3</sub>)<sub>6</sub>Cl<sub>3</sub>] and RNA constructs more highly favorable for alignment and docking of the two domains are used. In the construct that is shown, the normal hinge region between the two domains is replaced by six unpaired cytidines and a seven-base pair helix (J. E. Heckman and J. M. Burke, unpublished observations).

affect the substrate binding (19). Here, the same cleavage rates were observed when different ribozyme concentrations (100, 250, and 500 nM) were used, indicating that the rate measurements were carried out at saturating conditions for each of the active variants (data not shown).

Replacement of Mg<sup>2+</sup> with Co(NH<sub>3</sub>)<sub>6</sub><sup>3+</sup> generally enhances activity, particularly in the more severely inhibited variants (Figure 2B). Strikingly, almost full restoration of activity was achieved for C<sub>+1</sub>•G<sub>25</sub> when reaction conditions [Co(NH<sub>3</sub>)<sub>6</sub><sup>3+</sup>] and an RNA construct favoring proper alignment of the two domains were used (Figure 2C). These results establish that a base pair between positions +1 and 25 is required for catalytic function of the hairpin ribozyme. A structural model consistent with these observations is presented below. Using analogous combinations of base sub-

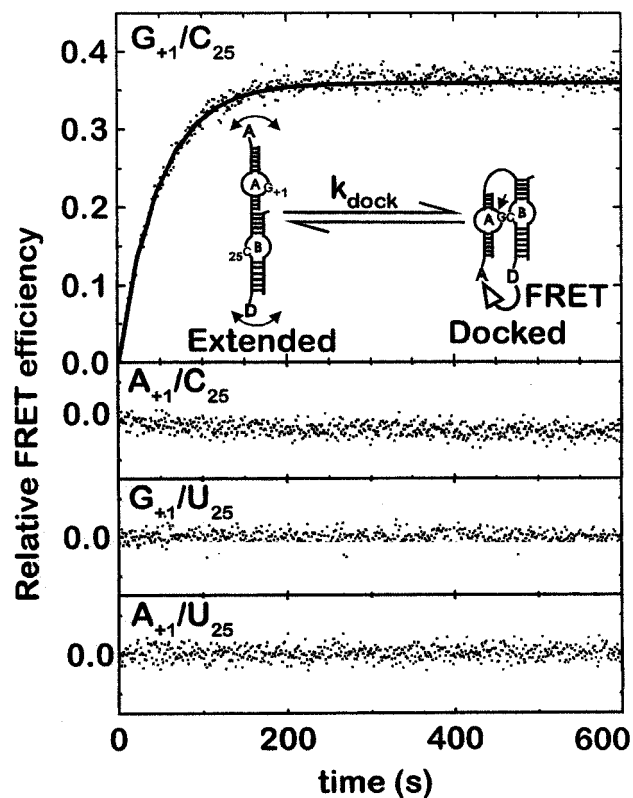


FIGURE 3: Global folding transition from an extended to a docked

stitution, we were unable to demonstrate covariation between position +1 or +2 in the substrate and position 24 or 26 of the ribozyme catalytic domain (data not shown).

Following substrate binding, the two domains interact with one another forming a docked complex, as previously shown by FRET (13) and footprinting (10) methods. The rate-limiting step of cleavage follows this docking event (13). Although the identity of the rate-limiting step is unknown, its pH independence suggests that it may be a post-docking conformational change, rather than reaction chemistry (13, 20). Some conditions (e.g., high concentrations of monovalent cations) strongly support cleavage, yet do not favor the formation of a stable docked complex (21). Analysis of the variants used in this study gave similar results, in that although activity was rescued, the stability of the docked complex is diminished in all active +1 and 25 variants, resulting in a population of docked molecules that is below the limit of detection of the FRET assay (Figure 3). Together, these results indicate that, following a transient docking step, the active variants can proceed to the transition state conformation leading to cleavage.

The interdomain base pair between positions +1 and 25 clearly serves as a key structural determinant of the reactive complex. MC-SYM models of the standard complex suggest that the G<sub>+1</sub>•A<sub>9</sub> sheared pair found within the ground state

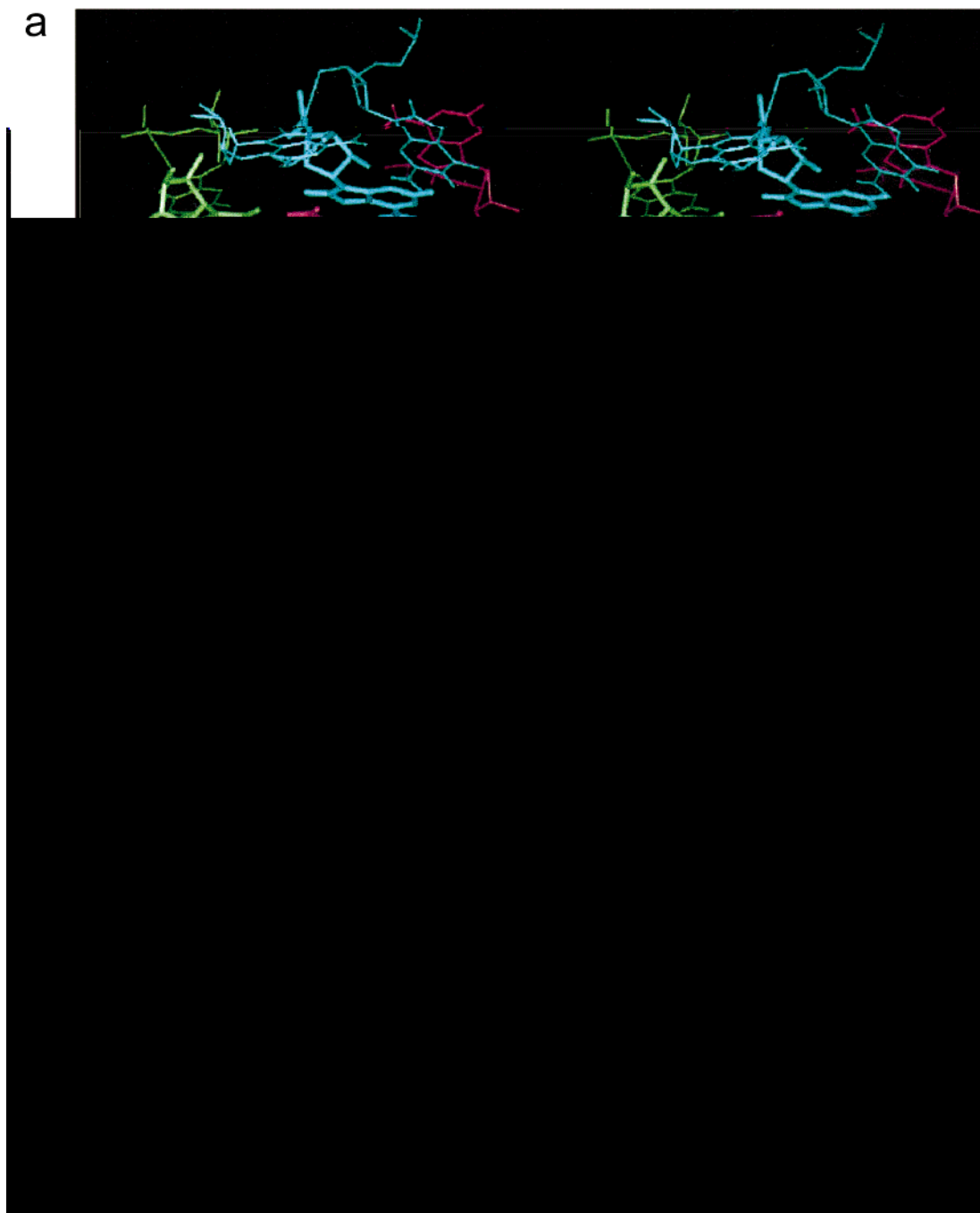


FIGURE 4: Molecular model of the  $A_9 \cdot G_{+1} \cdot C_{25}$  triplet. (a) Stereoview showing the proposed base triple interaction involving  $G_{+1}$  (red) and its partners  $A_9$  (blue) and  $C_{25}$  (green). The nucleotides immediately 5' and 3' of the triplet also are shown (thinner lines). (b) Secondary structure of the proposed base triple. Compensatory variants of the triplet analyzed in this work are also indicated. The potential formation of a Watson–Crick base pair between  $U_{+1}$  and  $A_9$  in the internal loop A may impair triplet formation and is consistent with the low level of restoration of cleavage activity of that combination (bottom).

structure of internal loop A (7) can readily accommodate formation of the  $G_{+1} \cdot C_{25}$  pair, which could lead to the formation of an  $A_9 \cdot G_{+1} \cdot C_{25}$  triplet (Figure 4a). This appealing hypothesis is currently under investigation in our laboratory. Interestingly, analogous triplets can be formed by the other active combinations, and the activities of the variants appear to correlate with their ability to adopt orthologous structures (Figure 4b). The very low activity observed for the  $U_{+1} \cdot A_{25}$  pair is consistent not only with the formation of a weak triplet but also with possible formation of a  $U_{+1} \cdot A_9$  pair that could disrupt the interdomain contact (Figure 4b).

The  $G_{+1} \cdot C_{25}$  base pair represents a useful starting point from which to build a tertiary structure model of the ribozyme–substrate complex. The proven interdomain contact between  $G_{+1}$  and  $C_{25}$  is also significant for targeted RNA cleavage by hairpin ribozymes, since targets are no longer limited to sequences containing a guanosine immediately 3' to the cleavage site.

#### ACKNOWLEDGMENT

We dedicate this paper to the memory of Robert Cedergren. We thank Ken Hampel, Molly Coseno, Sébastien

Lemieux, Patrick Gendron, and Nancy Bourassa for valuable comments and helpful discussions about the manuscript.

## REFERENCES

1. Walter, N. G., and Burke, J. M. (1998) *Curr. Opin. Chem. Biol.* 2, 24–30.
2. Butcher, S. E., Heckman, J. E., and Burke, J. M. (1995) *J. Biol. Chem.* 270, 29648–29651.
3. Komatsu, Y., Kanzaki, I., Koizumi, M., and Ohtsuka, E. (1995) *J. Mol. Biol.* 252, 296–304.
4. Komatsu, Y., Kanzaki, I., and Ohtsuka, E. (1996) *Biochemistry* 35, 9815–9820.
5. Shin, C., Choi, J. N., Song, S. I., Song, J. T., Ahn, J. H., Lee, J. S., and Choi, Y. D. (1996) *Nucleic Acids Res.* 24, 2685–2689.
6. Komatsu, Y., Shirai, M., Yamashita, S., and Ohtsuka, E. (1997) *Bioorg. Med. Chem. Lett.* 6, 1063–1069.
7. Cai, Z., and Tinoco, I. (1996) *Biochemistry* 35, 6026–6036.
8. Butcher, S. E., Allain, F. H., and Feigon, J. (1999) *Nat. Struct. Biol.* 6, 212–216.
9. Earnshaw, D. J., Masquida, B., Muller, S., Sigurdsson, S. T., Eckstein, F., Westhof, E., and Gait, M. J. (1997) *J. Mol. Biol.* 274, 197–202.
10. Hampel, K. J., Walter, N. G., and Burke, J. M. (1998) *Biochemistry* 37, 14672–14682.
11. Pinard, R., Heckman, J. E., and Burke, J. M. (1999) *J. Mol. Biol.* 26, 239–251.
12. Chowrira, B. M., Berzal-Herranz, A., and Burke, J. M. (1991) *Nature* 354, 320–322.
13. Walter, N. G., Hampel, K. J., Brown, K. M., and Burke, J. M. (1998) *EMBO J.* 17, 2378–2391.
14. Wincott, F., DiRenzo, A., Shaffer, C., Grimm, S., Tracz, D., Workman, C., Sweedler, D., Gonzalez, C., Scarinje, S., and Usman, N. (1995) *Nucleic Acids Res.* 25, 2677–2684.
15. Major, F., Turcotte, M., Gautheret, D., Lapalme, G., Fillion, E., and Cedergren, R. (1991) *Science* 253, 1255–1260.
16. Lemieux, S., Chartrand, P., Cedergren, R., and Major, F. (1998) *RNA* 4, 739–749.
17. Siwkowski, A., Shippy, R., and Hampel, A. (1997) *Biochemistry* 36, 3930–3940.
18. Schmidt, S., Beigelman, L., Karpeiski, A., Usman, N., Sorensen, U. S., and Gait, M. J. (1996) *Nucleic Acids Res.* 24, 573–581.
19. Walter, N. G., Albinson, E., and Burke, J. M. (1997) *Nucleic Acids Symp. Ser.* 36, 175–177.
20. Nesbitt, S. M., Hegg, L. A., and Fedor, M. J. (1997) *Chem. Biol.* 4, 619–630.
21. Murray, J. B., Seyhan, A. A., Walter, N. G., Burke, J. M., and Scott, W. G. (1998) *Chem. Biol.* 5, 587–595.
22. Chowrira, B. M., Berzal-Herranz, A., Keller, C. F., and Burke, J. M. (1993) *J. Biol. Chem.* 268, 19458–19462.

BI992024S